Natural Zeolite Polypropylene Composite Film Preparation and Characterization

F. ÖZMIHÇI, D. BALKÖSE, S. ÜLKÜ

Department of Chemical Engineering, Faculty of Engineering, Izmir Institute of Technology, Gaziosmanpasa Bulvari No.16, 35230 Cankaya/Izmir, Turkey

Received 3 November 2000; accepted 17 April 2001

ABSTRACT: In this research, the preparation and characterization of polypropylene (PP) and natural zeolite composites were studied. Natural zeolite mined in Gördes, Turkey was used as an alternative filler to $CaCO_3$. Films were prepared by the extrusion of PP, and surface-modified zeolite was made by polyethylene glycol 4000 with 2–4% zeolite. Zeolite-filled composites had densities between 0.73 and 0.83 g/cm^3 and had void fractions of 0.07–0.20. Although the permeability of water vapor through 2% zeolite-filled composites was very small, 4% zeolite-filled films had very high permeabilities. The yield stresses of 2–4% zeolite-containing films were around 26–27 N/mm^2 and were lower than that of PP, which indicated no adhesion between PP and zeolite. The effect of zeolite on the thermal degradation behavior in air and in a N_2 atmosphere was also studied. In air, zeolites did not cause the oxidation of PP. In a N_2 atmosphere, although the start of the thermal degradation of PP was retarded by zeolite, composites degraded at a faster rate than PP once the degradation started. At a processing temperature of 200°C, zeolites had no effect on the degradation of PP.
 J Appl Polym Sci 82: 2913–2921, 2001

Key words: poly(propylene) (PP); natural zeolites; water permeable; composite film; thermal degradation; crystallization; thermal properties

INTRODUCTION

Over the past several years, there has been increasing interest in the use of thermoplastics as matrices for composite materials. Fillers such as $CaCO_3$, silica, clays, and silver have been used in composite preparations. Extensive studies have been made of polypropylene (PP)–$CaCO_3$ composites.[1,2] PP, $CaCO_3$ filler, and an antioxidant were mixed to create a base sheet. $CaCO_3$ fillers were treated with a polyester plasticizer composed of adipic acid and propylene glycol. The antioxidant used was 2,6-di-*t*-butyl-4-methylphenol. PP powder, $CaCO_3$ filler, and the additives were well mixed in advance and then pelletized with the aid of a tandem-type extruder. The base sheet was stretched in the machine direction with two pairs of rollers with different rotating speeds and then stretched in the transverse direction with a pantogram-type biaxial stretching machine.[1] Galeski et al.[2] also studied $CaCO_3$–PP composites. Chalk-filled isotactic-PP (i-PP) composites were prepared from dried components. First, pellets of i-PP were wetted with the liquid modifier of an oligomer of ethylene oxide, and precipitated chalk was added and mixed until a uniform covering of the chalk particles with the oligomer of ethylene oxide was obtained. Second, chalk-filled i-PP was prepared by means of a twin screw extruder.

Correspondence to: F. Özmıhçı.

Journal of Applied Polymer Science, Vol. 82, 2913–2921 (2001)

The surface modification of $CaCO_3$ and some other fillers were studied by Domka.[3] The modifying substances were many types of surface-active substances, fatty acids and their derivatives, silane coupling agents, titanate coupling agents, and other metallorganic compounds and metallocenes. Specific organic oxyethylated compounds with long chains may serve the purpose well. Because of a relatively strong hydrophobization, in particular of the surface of chalk fillers, their modification with the previously mentioned compounds may lead to a considerable amount of polymer–$CaCO_3$ adhesion.[3]

Twin screw extruders were used for mixing the ingredients and drawing the films. Biaxial[1] or machine-direction stretching[4] of the extruded films caused splitting of the extruded PP phase at the periphery of the filler particles. Thus, a porous film permeable to gases was obtained. The empty space in the film scattered incident light, giving a pearlescent appearance. Pearlescent films with a nonporous PP surface layer and with a density of 0.65 g/cm^{-3} are present in the market.

PP degrades by the random homolytic cleavage of polymer chains, giving low-molecular-weight degradation products.[5] Horrocks and D'Souza[6] and Allen et al.[7] studied the thermooxidative degradation of PP. First-order degradation kinetics were assumed above 0.1 conversion. Antioxidants adsorbed to silica prior to blending and processing in PP films increased thermal stability of PP.[7] The metal content of silica accelerated the thermooxidative degradation of PP.

In this study, the preparation and characterization of PP–natural zeolite composites were studied. Natural zeolites mined in Gördes, Turkey were used as a substitute for $CaCO_3$. It was thought that in the pore structure of the zeolites would expand during extrusion and contribute to pore formation in the extruded films.

EXPERIMENTAL

Zeolitic tuffs from Gördes-Manisa, Turkey were used in the composite preparation. The characterization of the tuffs was done by Akdeniz.[8] The Brauner Emmet Teller (BET) surface area of the zeolitic tuff was 56 and 261 m^2/g from N_2 adsorption at 77 K and H_2O adsorption at 25°C, respectively.[8] The moisture adsorption capacity at 25°C of zeolite that was outgassed at 400°C for 4h at 10^{-5} torr was 13.6%.[9] The chemical composition was 10% Al_2O_3, 0.1% BaO, 1.5% CaO, 0.6% FeO, 1.4% K_2O, 0.9% MgO, 0.3%Na_2O, 77.5% SiO_2, and 22% H_2O.

Natural zeolite particles (2 μ) were obtained by the fractionation of ball-milled zeolite by sieving and sedimentation in water, respectively.

Surface modification was made by polyethylene glycol (PEG) 4000. It was made to prepare a homogenous dispersion and to prevent the agglomeration of particles in PP film. Modification was made by the method given by Domka.[3] The zeolite was mixed with 50% aqueous ethanol solution with 10% modifier. The zeolite solution ratio was taken as 1:0.3 on a weight:volume basis. The mixture was kneed at 40°C and then dried in a vacuum oven at 110°C under 400 mbar pressure for 3 h.

Petkim H418 PP (Izmir, Turkey) with a density of 0.89 g/cm^3 and an isotactic index of 0.75 was used in the experiments. It contained an antioxidant added in the plant.

PP films with 0–6% zeolite were prepared with extrusion with a Tonable Plastic Machinery extruder. The temperature of extrusion was 260°C; the length:diameter ratio was 24, and the screw speed was 550 rpm. The cast film was quenched by a polished drum cooled with water and was drawn by rollers with controlled speed.

Pure PP and films were characterized by Fourier transform infrared (FTIR) spectroscopy, differential scanning calorimetry (DSC), and thermogravimetric analysis (TGA). Ground zeolite particles were characterized by FTIR with the KBr disc method. We obtained DSC curves of the films by heating them at 10°C/min in the range of 25–300°C and then cooling the films to 25°C at 2°C/min in a Setaram DSC 92. The same heating and cooling program was applied to the films twice to examine the effect of prolonged heating on the films. We performed TGA analysis of the films by heating the films at 5–20°C/min in the range of 25–1000°C with a Shimadzu 51 thermogravimetric analyzer. A 15 mL/min N_2 flow rate was used in both DSC and TGA experiments.

Optical micrographs of zeolite, PP, modified zeolite, and composite films were taken both in reflection and transmission modes with an optical microscope fitted with an Olympus BX-60 and an Olympus CH40, respectively. The optical microscope was connected to Olympus PM-C35B camera.

The densities of the films were measured by Archimede's principle with the density kit of a Sartorius YDK 01 balance. The weight of the sam-

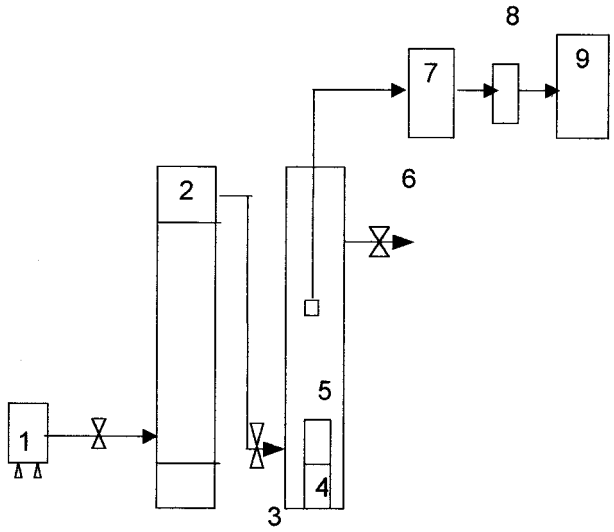

Figure 1 Permeability test apparatus: (1) air pump, (2) drierite column, (3) Cole–Palmer needle valves, (4) water, (5) test film, (6) Vaisala humidity probe, (7) Vaisala humidity meter, (8) RS232 interface, and (9) computer.

ple and the weight the water displaced by the sample were measured. The samples lighter than water were placed under a basket immersed in water to measure their weight in water. The samples heavier than water were placed on the basket to measure their density.

Mechanical testing of extruded films were performed with a Testometric AX M 500. Dog-bone-shaped samples were prepared according to the ASTM D-638 standard. The tensile tests on these films were carried out at a speed of 300 mm/min.

The permeability of films to water vapor were measured by the permeation test system described in Figure 1. The humidity of a 50 cm^3 volume ell was monitored by a Vaisala temperature and humidity tester. A glass bottle half filled with water and with a sealed test film on the mouth was placed in this cell. The cell was dried by sweeping with dry air obtained in a drierite column. The humidity of the cell versus time was recorded by a computer connected to a humidity meter by an RS232 interface, after isolation of the cell by the closure of Cole–Parmer needle valves at its inlet and outlet. The rate of permeation through the film was calculated from the initial humidity change with time, film area, and thickness with eq. (1).

$$P = (dQ/dt)(1/A)/\Delta p \quad (1)$$

where P is the permeability in $(cm^3/s)/(cm^2 cmHg)cm$, Q is the volume of the moles permeated under standard temperature and pressure, l and A are the membrane thickness and area, respectively, and Δp is the pressure difference between two sides of the film.

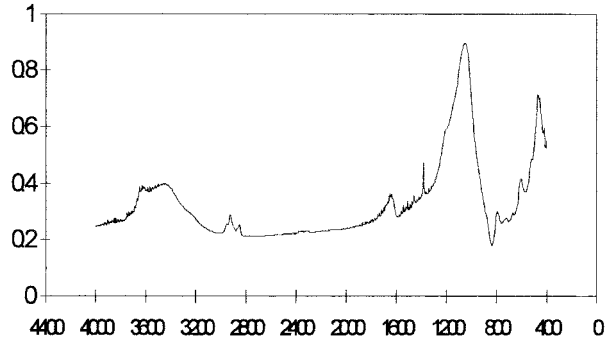

Figure 2 FTIR spectrum of Gördes zeolitic tuff.

RESULTS AND DISCUSSION

Zeolite Characterization

The apparent density of the pink-white Gördes zeolitic tuff was found to be 1.8 g/cm^3.

Peaks related with isolated and H-bonded OH stretching at 3700 and 3400 cm^{-1}, respectively; H_2O bending at 1620 cm^{-1}; T—O stretching at 1065cm^{-1}; external T—O at 790 cm^{-1}; and external and internal double-ring vibrations at 609 cm^{-1}were present in the IR spectrum of zeolite, as shown in Figure 2.[10,11]

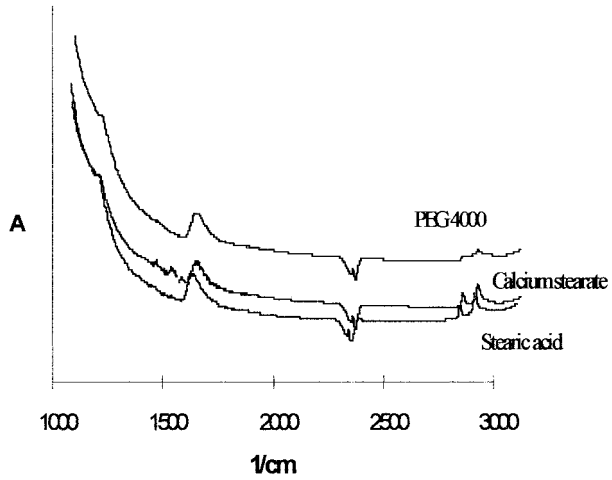

Figure 3 FTIR spectra of zeolites modified with calcium stearate, stearic acid, and PEG (4000).

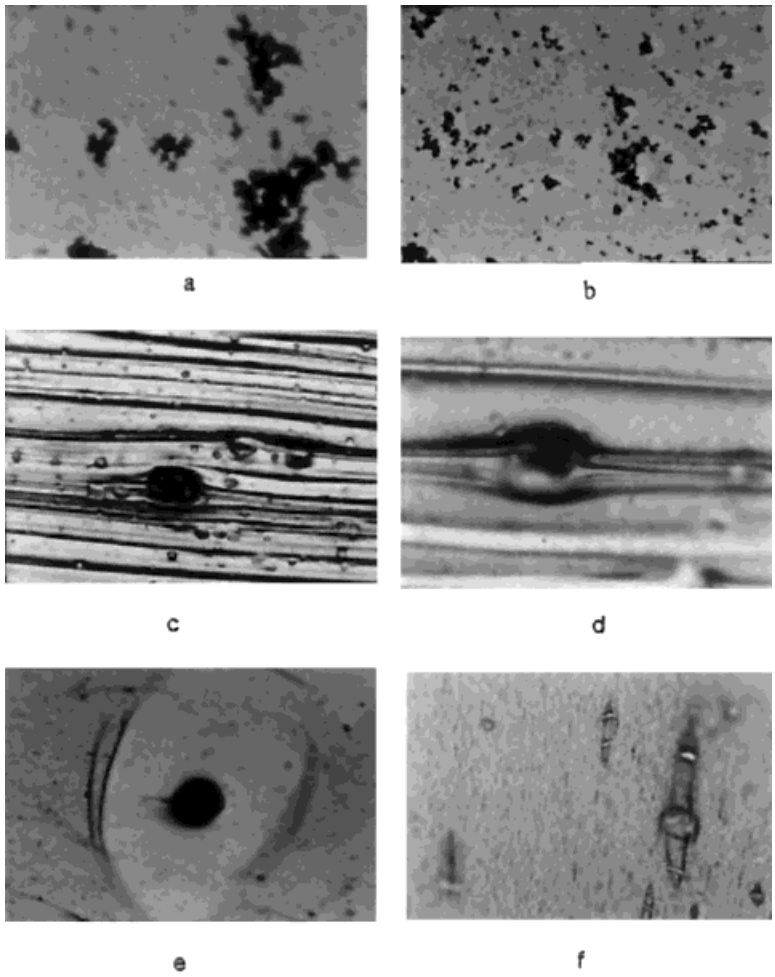

Figure 4 The optic micrograph of 75× magnified (a) pure natural zeolite and (b) PEG (4000)-modified natural zeolite, the transmitted optical micrographs of 2μ 6% zeolite-filled PP films: (c) 100× magnified composite film and (d) 250× magnified composite film, and tensile tested films: (e) 100× magnified and (f) 400× magnified taken with a transmitted optical micrograph.

Surface Modification

Natural zeolite is a hydrophilic inorganic material and has no chemical affinity to hydrophobic polymers. To avoid the agglomeration of zeolite in PP, it was modified with stearic acid, calcium stearate, or PEG 4000. The presence of modifiers was detected by FTIR spectroscopy. The peaks related to —CH_2 asymmetric stretching at 2930 cm^{-1} and symmetric stretching at 2970 cm^{-1} of the modifiers were present in the IR spectra of modified zeolites in Figure 3.

Stearic acid, calcium stearate, and PEG 4000-modified natural zeolite were examined with optical micrography. Because the size of the agglomerates was smaller in PEG 4000-modified zeolites than in unmodified zeolites, as shown in Figure 3, PEG 4000 was chosen as an appropriate modifier. The chemical reaction between zeolite is given in eq. (2):

$$\text{Zeolite} + \text{HO—}(\text{CH}_2\text{—CH}_2\text{—O—})_n\text{—H} \rightarrow \text{Zeolite—O—}(\text{CH}_2\text{CHO})_n\text{H} + \text{H}_2\text{O} \quad (2)$$

It was thought that O atoms of the PEG 4000 were directed toward zeolite particles. The transmitted optical micrograph of modified natural zeolite and pure natural zeolite are shown in Figure 4. As shown in Figure 4(a,b), the natural zeolite was agglomerated to the size of 600 μ, and after modification by PEG 4000, the agglomerations were broken to smaller sizes down to 6 μ. These

particles were fractionated below 2 μ size, but they stuck to each other to give larger particles. Even with PEG 4000 modification, 2 μ-size particles could not be observed under the microscope.

Film Characterization

Modified Gördes zeolite–PP extruded films had nonuniform thickness and had agglomerates of zeolites and tearings. Expansion of air from pores of zeolites on heating in an extruder and entrapment of them on quenching was another cause of void formation in the films. As the films were stretched, void formation occurred, and voids grew around the particles. When the zeolite particles were large, tearing of the film occurred. If the natural zeolite particles were smaller, no tearing would occur during stretching. The extruded films had nonuniform thickness, and for 2, 4, and 6% zeolite-filled PP films, thicknesses were in the range of 30–100, 50–80, and 30–50 μ, respectively. Distribution of filler was uneven, and agglomerations were observed, but no tearing occurred for 2–4% zeolites. For 6% zeolite, the films were thorns during extrusion. Fibers of composite rather than films were obtained in this case.

The spherical dark zeolite particles in air bubbles and the brighter underlayer PP were seen in optical microphotographs of the films shown in Figure 4(c). There were bubbles with zeolites at the center sized from 2–100 μ with in the films. In Figure 4(d), a view from thorn section of the film is shown.

Cold Drawing

The films from the extruder were stretched in the transverse direction by cold drawing in a tensile tester. Optical micrographs of the films with 4% zeolite and elongated 3.37 times in the stretching direction in the tensile tester are shown in Figure 4(e,f). The zeolite particle is dark and in the middle of the cavitations. The brighter part represents air bubbles in PP. The shapes of the bubbles were similar than those described by Nakamura et al.[4]

Density and Void Volume Fraction

The films had different densities at the beginning, in the middle, and at the end of extrusion runs because of the uneven mixing of zeolites and PP. The densities of the PP and zeolite were 0.89 and 1.8, respectively. The measured and predicted densities of the films from eq. (3) and their void volume fraction, as found from eq. (3), are given in Table I:

Table I Density of Zeolite-Filled PP Films

Zeolite Fraction	Thickness (mm)	Density (g/cm^3)	ε
2% (beginning)	0.01	0.87	0.02
2% (middle)	0.02	0.82	0.07
2% (end)	0.04	0.77	0.13
4% (beginning)	0.05	0.73	0.20
4% (middle)	0.02	0.87	0.04
4% (end)	0.03	0.73	0.20
6% (beginning)	0.05	0.83	0.10
6% (middle)	0.03	0.78	0.15

$$d_{ct} = (w_{pp} + w_z)/((w_{pp}/d_{pp}) + (w_z/d_z))$$
$$d_{ce} = (1 - \varepsilon) \cdot d_{ct} \quad (3)$$

where d and w are the density and weight fractions; the subscripts *PP* and *z* stand for PP and zeolite, respectively; ϵ is the closed void volume fraction; and the subscripts *c, e,* and *t* represent the composite, experimental, and theoretical values, respectively.

Table I shows that the densities of the composites (0.73–0.83 g/cm^3) were lower than the density of PP (0.89 g/cm^3) but higher than the density of the commercial pearlescent films (0.6 g/cm^3).

Uneven Mixing and Closed Pore Formation

The zeolite particles were smaller in size and had higher densities than the PP particles, so in the extrusion process, even if they were fed simultaneously, first the zeolites were introduced into the extruder and mixing occurred unevenly during extrusion process. The composites could not be stretched in the machine direction at high rates because the films were thorn when the zeolite content was high and the air bubbles exploded before PP was solidified, and thus, they were not entrapped in the films at the desired level. Thus, the densities of the composites were not as low as those of pearlescent films in the market.

Mechanical Properties

The mechanical properties of the extruded films are given in Table II. The yield stress (σ_c), yield strain, and elastic modulus (E_c) of the composites

Table II Mechanical Behavior of Extruded Films

Zeolite Fraction	Yield Stress (N/mm^2)	Yield Strain (%)	Stress at Break (N/mm^2)		Strain at Break (%)	Young Modulus	
			Exp.	Predicted		Exp.	Predicted
0	35	4.2	17.5	—	164	806	—
2%	26.1	3.7	6.3	43.3	204.5	406.2	686
4%	27.6	3.6	7.1	41.14	205	493.3	652

were lower than those of PP, as seen in Table II. The predicted values found from eqs. (4) and (5) were close to the experimental σ and E values, which confirmed that there was no adhesion between the filler and PP.

σ_c and E_c of a composite with void volume and with no adhesion between filler and matrix were as follows:

$$\sigma_c = \sigma_{pp}(1 - \varepsilon) \quad (4)$$

$$E_c = E_{pp}(1 - \varepsilon) \quad (5)$$

Although stress at break was lower for the composites, the strain at break increased because of presence of the void space as seen in Table II.

Permeability to Water Vapor

The permeability of PP and PP with 2% zeolite was very small for water vapor. On the other hand, PP with 4% zeolite had a very high permeability [1.5×10^{-5} (cm^{-3}/s)(cm^2cmHg)cm]. Its permeabilty was very close to that of natural leather 2.02×10^{-5}[(cm^{-3}/s)(cm^2cmHg)cm].[12] Thus, PP film with 4% zeolite can be used in packing where a high rate of water-vapor transmission is required. The high permeability of 4% zeolite film indicated the presence of open pores that allow the transmission of water vapor.

Melting and Crystallization

The effect of zeolite on the crystallization of PP during processing was investigated with DSC. The maxima of the melting endotherm and crystallization endotherms were 174 and 110°C for PP and the composites, respectively. As shown in representative DSC curves of the films in Figure 5, from the areas of the melting and crystallization endotherms, the heat of fusion (ΔH_f) and heat of crystallization (ΔH_c) of the films were obtained. Percent crystallinity of the films were found from ΔH_f or ΔH_c of the films and from the ΔH_f of 100% crystalline isotactic PP (209 J/g).[6] ΔH_f, ΔH_c, and % crystallinity of films are as reported in Table III. ΔH_f values in the range 63.8–87.9 J/g were obtained and were similar to the values found for $CaCO_3$-filled PP (60.9–65 J/g). ΔH_f for the first heating was a direct indication of the state of crystallinity of the films from the extruder. Although PP film was 30% crystalline, the composites had higher crystallinities (35–45%). Zeolite particles, acting as nucleating agents in PP crystallization, caused a higher crystallinity of PP in

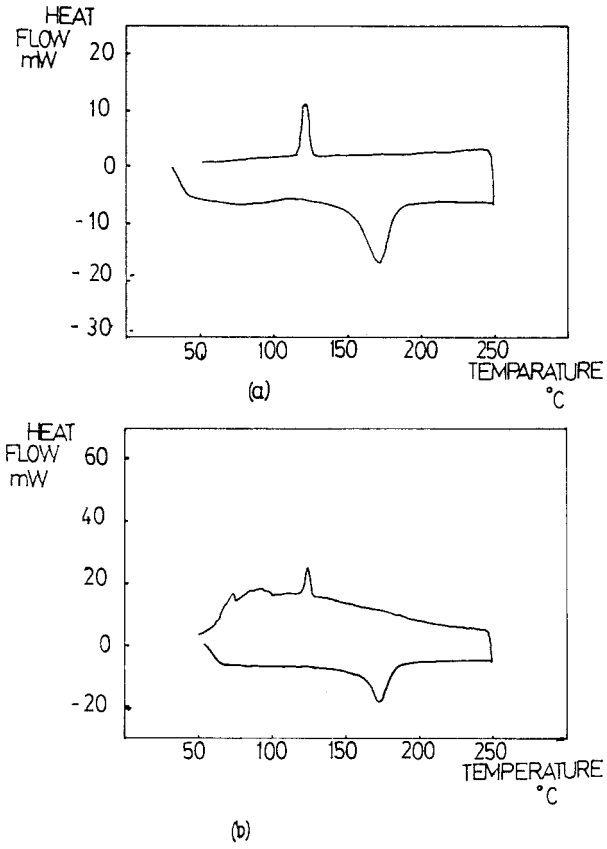

Figure 5 Zeolite (6%)-filled PP DSC curve.

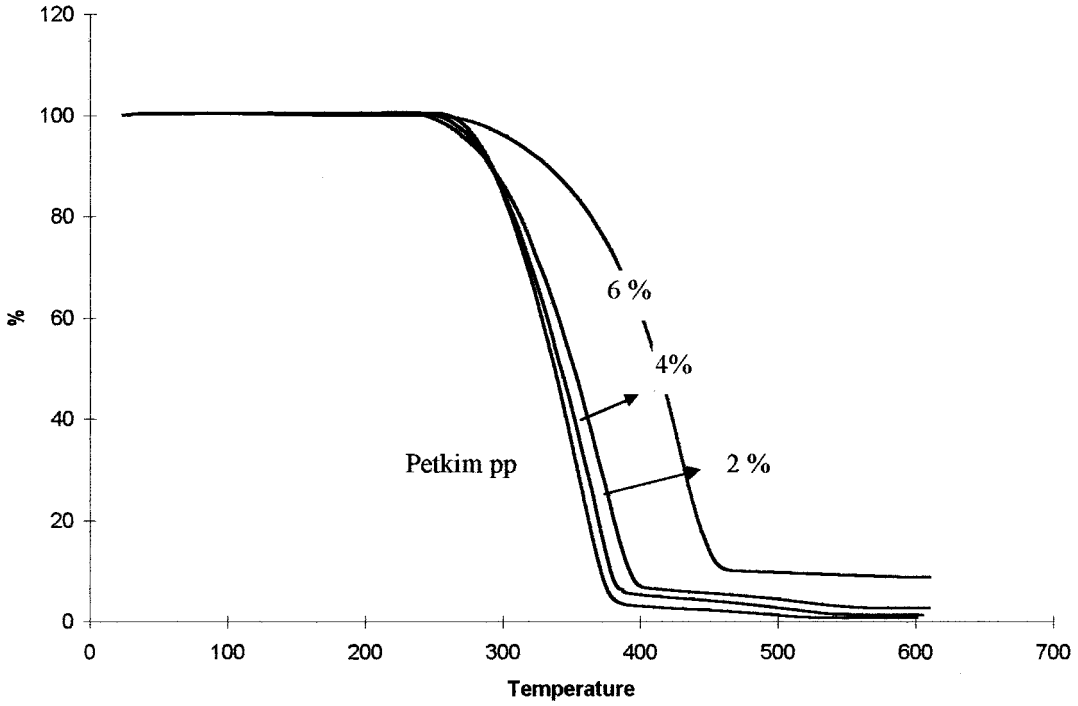

Figure 6 TGA curves of 2, 4, and 6% zeolite-filled PP composites.

the cooling system of the extruder. By cooling the molten PP at 2°C/min rate in DSC, we obtained similar crystallinities to those obtained in the extruder. PP and composites were crystallized to 26 and 38–40% respectively, which confirmed the behavior of zeolites as nucleating agents. Heating and cooling of the films with the same temperature program twice showed the stability of the films to heating and cooling cycles. Although a very low crystallinity (15%) was obtained for PP films, crystallinities of 2 and 4% zeolite-containing films were close to their values for the first heating. Films containing 6% zeolite were decomposed in the second heating cycle, and no melting or crystallization endotherms were present.

Thermal Degradation of PP

The effect of zeolite on the thermal degradation of PP at high temperatures was investigated by TGA. All the samples were heated to 1000°C at heating rate of 10°C/min. As shown in the TGA curves of the films in Figure 6, PP samples started to degrade at about 220°C. The composites started to degrade at least 10°C higher than pure PP. Zeolite retarded the onset of the thermal degradation of PP. Table IV gives the temperature of the start and termination of degradation, weight losses, and percentage of the remaining mass at the termination of degradation. Although PP lost 100% of its mass at

Table III Heat of Fusion, Heat of Crystallization, and Percent Crystallinity of the Films

	ΔH_f (kJ/kg)		ΔH_c (kJ/kg)		Crystallinity (%)			
Zeolite (%)	First Heating	Second Heating	First Cooling	Second Cooling	First Heating	Second Heating	First Cooling	Second Cooling
0	63.8	31.5	54.6	—	30	15	26	—
2	81.2	85.5	81.3	76.3	38	47	38	35
4	87.9	84.7	84.9	—	42	40	40	—
6	74.2	—	82.0	—	35	—	39	—

Table IV TGA Values Indicating Weight Loss Percent and Temperatures of 0–6% Zeolite Composites

Zeolite Fraction (%)	Temperature (°C)		Weight Loss (% at Termination of Degradation)	Remaining Mass (%)
	Start of Degradation	Termination of Degradation		
0 (Petkim PP)	220	550	100	0
2	230	575	99	1
4	230	575	98	2
6	240	575	91	9

600°C, zeolite had only lost only its water at that temperature. Remaining masses for 2, 4, and 6% zeolite-filled composites were 1, 2, and 9%, respectively, as shown in Table IV. These values were different than the expected values of 2, 4, and 6%.This indicated an uneven dispersion of zeolite in the films.

PP and 6% zeolite-filled films were heated at different heating rates; the TGA curves are given in Figure 7. All samples started degradation at about 230°C at different heating rates.

Degradation kinetic analysis of Petkim PP and 6% zeolite-filled composites were made with the TGA kinetic analysis software of a Shimadzu 51 thermogravimetric analyzer. The kinetic analysis software, based on the Ozawa principle, found the activation energy (E_a), frequency factor (A), and order (L) for the degradation reaction. Volatilization of degradation products is an important property, and L gives information about minimum degree of polymerization of volatile degradation products. Equation (6) shows an example of the homolytic cleavage of PP by heat and the difference between volatile and nonvolatile materials:

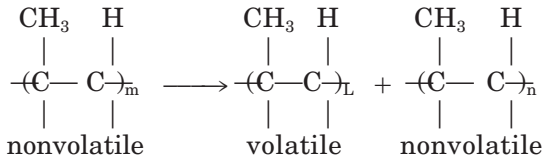

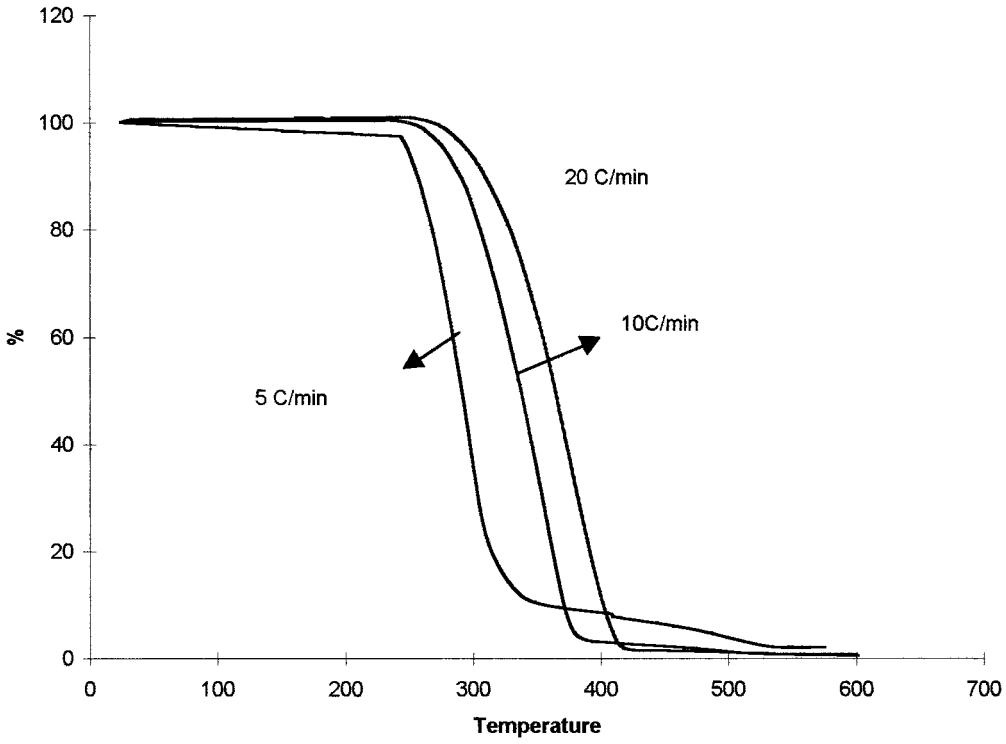

Figure 7 TGA analysis of a 6% zeolite-filled extruded PP film at different heating rates.

Table V Kinetic Analysis of Thermal Degradation

	E (kcal/mol)	n	A (L/min)	$k \times 10^3$ (L/min)
Petkim PP	59.34	4.9	2.39×10^3	3.4
6% Zeolite-filled extruded film	42.90	5.0	5.88×10^2	30

$$m = L + n \quad n > L \tag{6}$$

If the degree of polymerization of degraded polymer is lower than a critical L value, it is volatile. For PP, L was around 5. K, the rate constant of the first-order degradation reaction, was calculated as 250°C from the Arrhenius equation; this is also reported in Table V.

As shown in Table V, for PP and for 6% zeolite-filled extruded PP film, the E_a's were 59.34 and 42.90 kcal/mol respectively. Zeolite decreased the E_a of PP degradation.

The degree of polymerization of volatile polymer L was nearly the same for pure PP and zeolite added PP. Although zeolite retarded the onset of the thermal degradation of PP, it accelerated the degradation of PP because a higher k value was found for zeolite-filled PP. This may have been due to the presence of 0.6% FeO in the zeolite as the silica with Fe also caused faster degradation of PP.[7]

CONCLUSIONS

Zeolitic tuff from Gördes was used as an alternative material to obtain porous and permeable PP films. Efficient mixing of zeolite and PP with compounding extruders and then the film extrusion would give better distribution of fillers and voids around fillers. The crystallinity of the films with zeolite were higher than PP because zeolites act as nucleating agents. Although the start of the thermal degradation of PP was retarded by zeolite, PP with zeolite degraded at faster rate than pure PP once the degradation started.

REFERENCES

1. Nago, S.; Nakamura, S.; Mizutani, Y. J Appl Polym Sci 1992, 45, 1527.
2. Galeski, A.; Kryszewski, M.; Kawolewski, T. Polym Eng Sci 1992, 32, 1217.
3. Domka, L. Colloid Polym Sci 1994, 272, 1190.
4. Nakamura, S.; Kaneko, S.; Mizutani, Y. J Appl Polym Sci 1993, 49, 143.
5. Fried, J. R. Polymer Science and Technology; Prentice Hall: NJ, 1995.
6. Horrocks, A. R.; D'Souza, J. A. J Polym Sci A 1991, 42, 243.
7. Allen, N. S.; Edge, M.; Coralles, T.; Childs, A.; Liauw, C.; Catalina, F.; Peinado, C.; Minihan, A. Polym Degrad Stab 1997, 56, 217.
8. Akdeniz, Y. M.S. Thesis, Izmir Institute of Technology, 1999.
9. Ülkü, S.; Balköse, D.; Özmıhçı, F.; Akdeniz, Y.; Negis, F. Presented at Industrial Raw Materials Symposium, Izmir, Turkey, 1999.
10. Goryainov, S. V.; Stolpovskaya, V. N.; Likhacheva, A. Y.; Belitsky, I. A.; Fursenko, B. A. Nat Zeolites Congress 1995, 245. Eds: Mumpton, F. A., Collela, C., Lit Editrice A. De Frede via Mezzocannonen 69, Iscia, Naples, Italy.
11. Krivacsy, Z.; Hlavay, J. Zeolites 1995, 15, 551.
12. Ulutan, S.; Balköse, D. J Membr Sci 1996, 115, 217.